LA-UR-00 - 4678

97801

Approved for public release;
distribution is unlimited

Title: **Fundamental Studies of Radiation Damage in Two-Phase Oxide Composites**

Author(s): *Kurt E. Sickafus
Enrique Pifarre Montaner
James A. Valdez
Licia Minervini
Robin W. Grimes
Jeremy N. Mitchell
Thomas Hartmann
Kenneth J. McClellan

Submitted to: DOE Office of Scientific and Technical Information (OSTI)

Los Alamos
NATIONAL LABORATORY

Form 836 (10/96)
ST 2629

DISCLAIMER

Fundamental Studies of Radiation Damage in Two-Phase Oxide Composites

*Kurt E. Sickafus (MST-8)

Enrique Pifarre Montaner (Ecole Europeenne d'Ingenieurs en Genie the Materiaux, SPAIN)

James A. Valdez (MST-8)

Licia Minervini (Imperial College, U.K.)

Robin W. Grimes (Imperial College, U.K.)

Jeremy N. Mitchell (NMT-16)

Thomas Hartmann (E-ET)

Kenneth J. McClellan (MST-8)

Abstract

This is the final report of a three-year, Laboratory-Directed Research and Development (LDRD) project at the Los Alamos National Laboratory (LANL). The goal of this project was to increase our fundamental understanding of radiation-induced damage in multi-phase ceramic oxide materials, with component phases having different radiation tolerances and mechanical properties. Almost all of our knowledge of radiation damage behavior in ceramics derives from experiments performed on single-phase materials. This project is dedicated to obtaining information on damage evolution in two-phase ceramic systems. Applications for such composites include rock-like, oxide waste-forms or nuclear fuel-forms for the immobilization and/or destruction of plutonium and higher actinides, as well as the immobilization of high-level radioactive wastes.

Background and Research Objectives

In the course of this project, we have identified a particularly intriguing application for ceramic composites: rock-like, oxide waste-forms or nuclear fuel-forms for the immobilization and/or destruction of plutonium and higher actinides, as well as the immobilization of high-level radioactive wastes. Candidate materials for these applications must be: (1) chemically durable; (2) able to accommodate actinide species in their structures; and (3) be highly tolerant to damage from exposure to radiation.

We have selected a set of candidate oxides for matrix phases for composite waste-forms and fuel-forms, based on the criteria of chemical durability and radiation resistance. These include: spinel ($MgAl_2O_4$), rutile (TiO_2), geikielite ($MgTiO_3$), and cubic-stabilized zirconia (ZrO_2). We have also identified oxides in the pyrochlore family ($A_2B_2O_7$ compounds) as candidate host phases for actinides in our proposed ceramic composite wasteforms.

---

*Principal Investigator, e-mail: currier@lanl.gov

Importance to LANL's Science and Technology Base and National R&D Needs

This project will benefit the Environmental Management program at Los Alamos National Laboratory (LANL). The EM program at LANL seeks to strengthen, promote, and expand Los Alamos environmental competencies using technical expertise developed for its mission of reducing the nuclear danger.

Scientific Approach and Accomplishments

Introduction

In this project, we developed a new ceramic-ceramic composite consisting of the mineral geikielite ($MgTiO_3$) as a matrix phase and the mineral pyrochlore ($Er_2Ti_2O_7$) as a minor, second phase. We conceived of this material for use as a possible nuclear waste-form for the immobilization and storage of surplus actinides or high-level radioactive wastes. Previous studies have shown that geikielite, $MgTiO_3$ ($R\bar{3}$) has good radiation damage tolerance[1]. The temperature dependence of ion irradiation damage indicates that annealing mitigates the effects of point defects introduced into the structure by atomic collisions. However, geikielite is a nearly close-packed oxide and generally, only small cations fit into its structure. $Er_2Ti_2O_7$ is a cubic pyrochlore (Fd3m), a compound in the more general rare-earth (RE) family of compounds with composition $(RE)_2Ti_2O_7$. Pyrochlores are generally not as radiation tolerant as oxides such as geikielite, but they have a relatively open structure that can accommodate large cations such as actinides. This makes pyrochlores an important constituent in a composite designed to incorporate actinides and to resist self-damage due to alpha particle decay. Our titanate-based geikielite-pyrochlore composites (like SYNROC) may be useful for the encapsulation of high level radioactive wastes, by combining the radiation damage resistance of geikielite and the capability to host surplus actinides in the pyrochlore structure.

In this project, we performed radiation damage experiments on composite $MgTiO_3$ - $Er_2Ti_2O_7$ samples (at a temperature of about 120K) using 350 keV Xe^{++} ions to ion fluences ranging from 1×10^{14} to 1×10^{16} Xe/cm^2. Irradiated samples were analyzed using transmission electron microscopy (TEM) and nano-indentation techniques

(in the latter case, the Young's modulus and hardness of the implanted samples were measured). Observations of irradiated samples were also made using light microscopy.

Experimental Procedure

The samples used in this study were: (1) a single crystal of $MgTiO_3$,; (2) a single crystal of $Er_2Ti_2O_7$; and (3) a crystalline composite sample with composition $MgTiO_3$ – 95 mol.% and $Er_2Ti_2O_7$ – 5 mol.%. All crystals were grown using a Crystal Systems Inc. floating-zone crystal growth unit in the Single Crystal Growth Laboratory at Los Alamos National Laboratory. The three crystal samples described above were cut to dimensions of approximately $10 \times 10 \times 0.5$ mm and polished on one side to a mirror finish.

Ion-beam experiments were conducted in the Ion Beam Materials Laboratory (IBML) at LANL. All samples were irradiated with 350 KeV Xe^{++} ions. Ion fluences ranged from 10^{14} to 10^{16} Xe^{++}/cm^2. Prior to irradiation, each sample was cooled to a temperature of about 120K using liquid nitrogen conduction cooling. Temperature excursions during irradiations were about ± 5 K, as measured using a thermocouple. The Xe^{++} ion doses used in this experiment, in units of Xe^{++}/cm^2, were: (a) 10^{14}, (b) 2.5×10^{14}, (c) 5×10^{14}, (d) 7.5×10^{14}, (e) 10^{15}, (f) 2.5×10^{15}, (g) 5×10^{15}, (h) 7.5×10^{15}, (I) 10^{16}. Three un-irradiated substrates of $MgTiO_3$, $Er_2Ti_2O_7$, and the composite $MgTiO_3$ - $Er_2Ti_2O_7$, were used as controls for the experiments.

The Monte Carlo code TRIM [2] was used to estimate the ion range and the profile of displacement damage in the Xe-ion irradiation experiments. The projected range and the damage peak of 350 KeV Xe^{++} ions, for a 5° angle of incidence, were estimated to be 170 nm, using a density of 7.045 g/cm^3 for $Er_2Ti_2O_7$ pyrochlore and 180nm, using a density of 3.89 g/cm^3 for $MgTiO_3$. The damage level in the peak damage region was estimated to be 13 displacements per atom (dpa) for pyrochlore and 23 dpa for geikielite, for the largest dose of this study: 1×10^{16} Xe^{++}/cm^2.

Some of the irradiated composite $MgTiO_3$ - $Er_2Ti_2O_7$ samples were prepared in cross section for examination by transmission electron microscopy (TEM). The radiation-induced microstructures were examined in a Philips CM-30 electron microscope operating at 300 keV. Bright-field (BF) imaging and microdiffraction techniques were used in the TEM analyses. Other characterization of irradiated samples included light microscopy, high resolution transmission electron microscopy (HRTEM), and X-ray diffraction (XRD).

Nano-indentation (or ultramicrohardness) was used to investigate the near-surface mechanical properties of the irradiated samples.

In these experiments, a Nano Indenter® II instrument at LANL was used to determine the Young's modulus (E) and the hardness (H), by the continuous stiffness method [3].

In this method, the applied load and the indenter displacement are continuously increased in each indentation test. The load range for these experiments was approximately 0-4 mN, with a maximum displacement of 100 nm. The latter choice was made in order to avoid influences from the un-implanted substrate. A fused silica sample was used as a control sample for these experiments.

Results and discussion

Fig. 1 shows cross-sectional TEM results obtained from a $MgTiO_3$ - $Er_2Ti_2O_7$ composite sample irradiated at 120 K with 350 keV Xe^{++} ions to a fluence of 5×10^{14} Xe^{++}/cm^2. The top image in Fig. 1 is a bright-field (BF) micrograph obtained from a pyrochlore precipitate located at the surface of the implanted sample, while the bottom BF micrograph was obtained from a region of implanted geikielite matrix. The arrows on the left side of the BF images indicate the direction of the incident Xe^{++} ions. Each arrow also points directly to the top surface of the respective phases. It should be noted that the thickness of a typical pyrochlore precipitate, impinging on the surface of the irradiated composite sample, was very much greater than the depth of the implantation (precipitates were at least several microns thick).

A continuous amorphous layer was found in the ion irradiated region of the $Er_2Ti_2O_7$ pyrochlore precipitate (Fig. 1). The fact that the irradiated region is amorphous was confirmed using micro-diffraction (results not shown here). The thickness of the amorphous pyrochlore layer is about 180 nm, i.e. about 10 nm greater the projected range for 350 keV Xe^{++} ions in $Er_2Ti_2O_7$, as estimated using TRIM simulations. For geikielite, TRIM simulations regarding the thickness of the implanted layer agree with TEM observations. Both TRIM and TEM (Fig. 1) indicate that the thickness of the implanted layer is about 180 nm.

In the lower BF image in Fig. 1, obtained from the $MgTiO_3$ geikielite matrix, regions of two different contrast are apparent in the ion irradiated region. The micro-diffraction pattern from this region (shown as an inset in Fig. 1) suggests that the implanted area is crystalline. Nevertheless, HRTEM observations were made in this region in order to better assess the structure of the irradiated layer in regions containing the geikielite matrix. Figure 2 shows an HRTEM image (Fig. 2a) and a TEM-BF image (Fig. 2b) obtained from a region of irradiated geikielite matrix.

Some of the small dark-contrast features in the BF image (Fig. 2b) are found to be crystalline in the HRTEM image (these regions exhibit lattice fringes in Fig. 2a). The remaining light-contrast areas in Fig. 2b are primarily amorphous, as determined by the absence of fringes in the HRTEM image (Fig. 2a).

For the ion fluence of $5 \cdot 10^{14}$ Xe/cm^2 in Figs. 1 & 2, the peak displacement damage dose for the $MgTiO_3$ is estimated (by TRIM) at ~1.1 dpa, while for $Er_2Ti_2O_7$, the peak displacement damage is about 0.65 dpa. Under the 120K irradiation condition used in these experiments, this dose renders the pyrochlore phase fully amorphous, while the geikielite phase is partially amorphized. Both of these observations are in reasonable agreement with previous observations on pure geikielite and pure pyrochlore. Mitchell et al. [1] observed fully-amorphized $MgTiO_3$ by a peak dose of about 2.7 dpa, for irradiations at 170K using 400 keV Xe^{++} ions. No observations of the radiation response of pure $Er_2Ti_2O_7$ have been published. However, Wang et al. [4] observed amorphization of a similar pyrochlore, $Gd_2Ti_2O_7$, by a dose of ~0.4 dpa at 200K using 0.6 MeV Ar^+ ions. These results suggest that no enhancement in radiation resistance is gained by incorporating the pyrochlore phase in a composite. Both the pyrochlore and the geikielite phases amorphize at approximately the same rates in the composite as they do in their monolithic forms.

Figure 3 shows results obtained from nano-indentation experiments on unirradiated and irradiated samples of: (1) geikielite single crystal; (2) $Er_2Ti_2O_7$ pyrochlore single crystal; and (3) a geikielite - $Er_2Ti_2O_7$ pyrochlore composite. The plots in Fig. 3 show how Young's modulus and hardness vary with Xe^{++} ion fluence, for an indenter displacement of 80 nm. These plots were obtained using measured E and H values at fixed indenter displacement, in load-displacements measurements on each sample. The standard deviation of the measurements is also shown in Fig. 3. The results presented in Fig. 3 represent a rather unique nanoindentation behavior for irradiated ceramics. For geikielite, pyrochlore, and the composite, both E and H exhibit an initial decrease with increasing Xe ion fluence, followed by some recovery at high dose. At the highest Xe ion doses in Fig, 3, both the geikielite and pyrochlore phases are fully-amorphized. It is expected that amorphous phases will exhibit the lowest moduli and hardnesses. This is observed in Xe-ion irradiated spinel ($MgAl_2O_4$), for instance [5]. Reasons for the recovery of E and H at high ion fluence are unclear at this time.

Conclusion

We have developed a new ceramic-ceramic composite consisting of the mineral geikielite ($MgTiO_3$) as a matrix phase and the mineral pyrochlore ($Er_2Ti_2O_7$) as a minor, second phase.

The geikielite exhibits higher radiation tolerance than the pyrochlore phase in the composite, but the pyrochlore phase is an important constituent because it serves as an actinide host phase. There seems to be no enhancement (or degradation) in the radiation resistance of either the geikielite or the pyrochlore phases when placed in a composite environment. The work performed on this project represents one of the first documented attempt to measure the radiation damage response of a ceramic oxide composite. This is a very important new area for research in which we have clearly only scratched the surface.

Publications

[1] Pifarre Montaner, E. and K. E. Sickafus, "Irradiation Effects in $MgTiO_3$-$Er_2Ti_2O_7$ Ceramic Composites," Ceram. Trans., submitted for publication, (2000).

[2] Minervini, L., R. W. Grimes and K. E. Sickafus, "Disorder in Pyrochlore Oxides," J. Am. Ceram. Soc., in press, (2000).

[3] Li, F., M. Ishimaru, P. Lu, I. V. Afanasyev-Charkin and K. E. Sickafus, "Damage Evolution in Xe-Ion Irradiated Rutile (TiO_2) Single Crystals," Nucl. Instr. and Meth. in Phys. Res. B, in press, (2000).

[4] Li, F., P. Lu, M. Ishimaru and K. E. Sickafus, "Effect of heavy ion irradiation on near-surface microstructure in single crystals of rutile TiO_2," J. Nucl. Mater., submitted for publication, (2000).

[5] Sickafus, K. E., R. J. Hanrahan, Jr., K. J. McClellan, J. N. Mitchell, C. J. Wetteland, D. P. Butt, P. Chodak, III, K. B. Ramsey, H. T. Blair, K. Chidester, H. Matzke, K. Yasuda, R. A. Verrall and N. Yu, "Burn and Bury Option for Plutonium," Ceram. Bull., **78 (1)**, 69-74, (1999).

[6] Li, F., P. Lu, K. E. Sickafus, C. R. Evans and M. Nastasi, "Damage Evolution in Xe-Ion Irradiated Rutile (TiO_2) Single Crystals," Mater. Res. Soc. Symp. Proc., **540** 311-316, (1999).

[7] Hartmann, T., L. M. Wang, W. J. Weber, N. Yu, K. E. Sickafus, J. N. Mitchell, C. Wetteland, J., M. Nastasi, M. G. Hollander, N. P. Baker, C. R. Evans, J. R. Tesmer and C. J. Maggiore, "Ion Beam Radiation Damage Effects in Rutile (TiO_2)," Nuclear Instruments and Methods in Physics Research B, **141** 398-403, (1998).

[8] Devanathan, R., W. J. Weber, K. E. Sickafus, M. Nastasi, L. M. Wang and S. X. Wang, "Cryogenic radiation response of sapphire," Nuclear Instruments and Methods in Physics Research B, **141** 366-377, (1998).

[9] Devanathan, R., K. E. Sickafus, W. J. Weber and M. Nastasi, "Effects of Ionizing Radiation in Ceramics," J. Nucl. Mater., **253** 113-119, (1998).

[10] Sickafus, K. E., "The Complementary Nature Of Electron Microscopy And Ion Channeling For The Assessment Of Radiation Damage Evolution In Ceramics," in Microscopy and Microanalysis '98, edited by G. W. Bailey, K. B. Alexander, W. G. Jerome, M. G. Bond and J. J. McCarthy (Springer-Verlag, New York, Inc., Atlanta, Georgia, July 12-16, 1998, 1998), Vol. 4, Supplement 2, pp. 558-559.

[11] Mitchell, J. N., R. Devanathan, N. Yu, K. E. Sickafus, C. Wetteland, J., V. Gopalan, M. Nastasi and K. J. McClellan, "Radiation Effects in Corundum Structure Derivatives," Nuclear Instruments and Methods in Physics Research B, **141** 461-466, (1998).

[12] Mitchell, J. N., N. Yu, R. Devanathan, K. E. Sickafus, M. Nastasi and K. J. McClellan, "Radiation-Induced Phase Transformations in Ilmenite-Group Minerals," in New Directions in Transmission Electron Microscopy & Nano-Characterization of Materials: Proceedings of the Asian Science Seminar in Commemoration of the 20th Anniversary of the HVEM Laboratory of Kyushu University, , edited by C. Kinoshita, Y. Tomokiyo and S. Matsumura (Kyushu University Press, Fukuoka, Japan,), pp. 267-276(1998).

[13] Mitchell, J. N., N. Yu, R. Devanathan, K. E. Sickafus, M. Nastasi and G. L. Nord, Jr., "Ion irradiation damage in ilmenite at 100 K," Nucl. Instr. and Meth. B, **127/128** 629-633, (1997).

[14] Devanathan, R., K. E. Sickafus, W. J. Weber, J. N. Mitchell and M. Nastasi, "Radiation Response of $FeTiO_3$, $MgTiO_3$, and α-Al_2O_3," Materials Science & Engineering, **A253** 131-134, (1997).

[15] Mitchell, J. N., N. Yu, K. E. Sickafus, M. Nastasi, T. N. Taylor, K. J. McClellan and G. L. Nord, Jr., "A Comparative Study of Radiation Damage in Al_2O_3, $FeTiO_3$, and $MgTiO_3$," Mater. Res. Soc. Symp. Proc., **396** 173-178, (1996).

References

[1] Mitchell, J. N., N. Yu, K. E. Sickafus, M. Nastasi and K. J. McClellan, "Ion Irradiation Damage in Geikielite ($MgTiO_3$)," Phil. Mag. A, 78 (3), 713-725, (1998).

[2] Ziegler, J. F., J. P. Biersack and U. Littmark, "The Stopping and Range of Ions in Solids," Book The Stopping and Range of Ions in Solids, 1, (1985).

[3] Oliver, W. C. and G. M. Pharr, "An improved technique for determining hardness and elastic modulus using load and displacement sensing indentation experiments," J. Mater. Res., 7 (6), 1564-1583, (1992).

[4] Wang, S. X., L. M. Wang, R. C. Ewing, G. S. Was and G. R. Lumpkin, "Ion irradiation-induced phase transformation of pyrochlore and zirconolite," Nucl. Instr. and Meth. in Phys. Res. B, 148 704-709, (1999).

[5] Sickafus, K. E., C. J. Wetteland, N. P. Baker, N. Yu, R. Devanathan, M. Nastasi and N. Bordes, "A Comparison Between the Irradiation Damage Response of Spinel and Zirconia due to Xe Ion Bombardment," Materials Science & Engineering, A253 78-85, (1998).

Figure Captions

Figure 1: Transmission electron microscopy (TEM) bright-field (BF) images obtained from an $MgTiO_3 - Er_2Ti_2O_7$ composite sample irradiated with 350 keV Xe^{++} ions (top BF image from an $Er_2Ti_2O_7$ pyrochlore precipitate; bottom BF image from a region of $MgTiO_3$ geikielite matrix; bottom inset microdiffraction pattern from a region of geikielite matrix) (ion fluence = 5×10^{14} Xe^{++}/cm^2; irradiation temperature = 100 K). Also shown are results of Monte Carlo simulations (based on the computer code TRIM) showing the range of 350 keV Xe^{++} ions in $MgTiO_3$ and $Er_2Ti_2O_7$, respectively, as well as displacement damage distributions for Xe ions in both oxide phases.

Figure 2: (a) High-resolution transmission electron microscopy (HRTEM) image and (b) cross-sectional TEM image obtained from a region of $MgTiO_3$ phase in an $MgTiO_3 - Er_2Ti_2O_7$ composite sample (same sample as in Fig. 1 irradiated with 350 keV Xe^{++} ions to. a fluence of 5×10^{14} Xe^{++}/cm^2 at 100 K. At this dose, the irradiated $MgTiO_3$ consists of isolated crystalline regions in an amorphous matrix.

Figure 3: (a) Young's modulus (E) and (b) hardness (H) as a function of 350 keV Xe^{++} ion fluence for three different samples: (1) $MgTiO_3$ (Geikieliete); (2) $Er_2Ti_2O_7$ (Pyrochore) and (3) an $MgTiO_3$ - $Er_2Ti_2O_7$ composite sample. Measurements were made using the nanoindentation technique with an 80 nm indenter displacement.

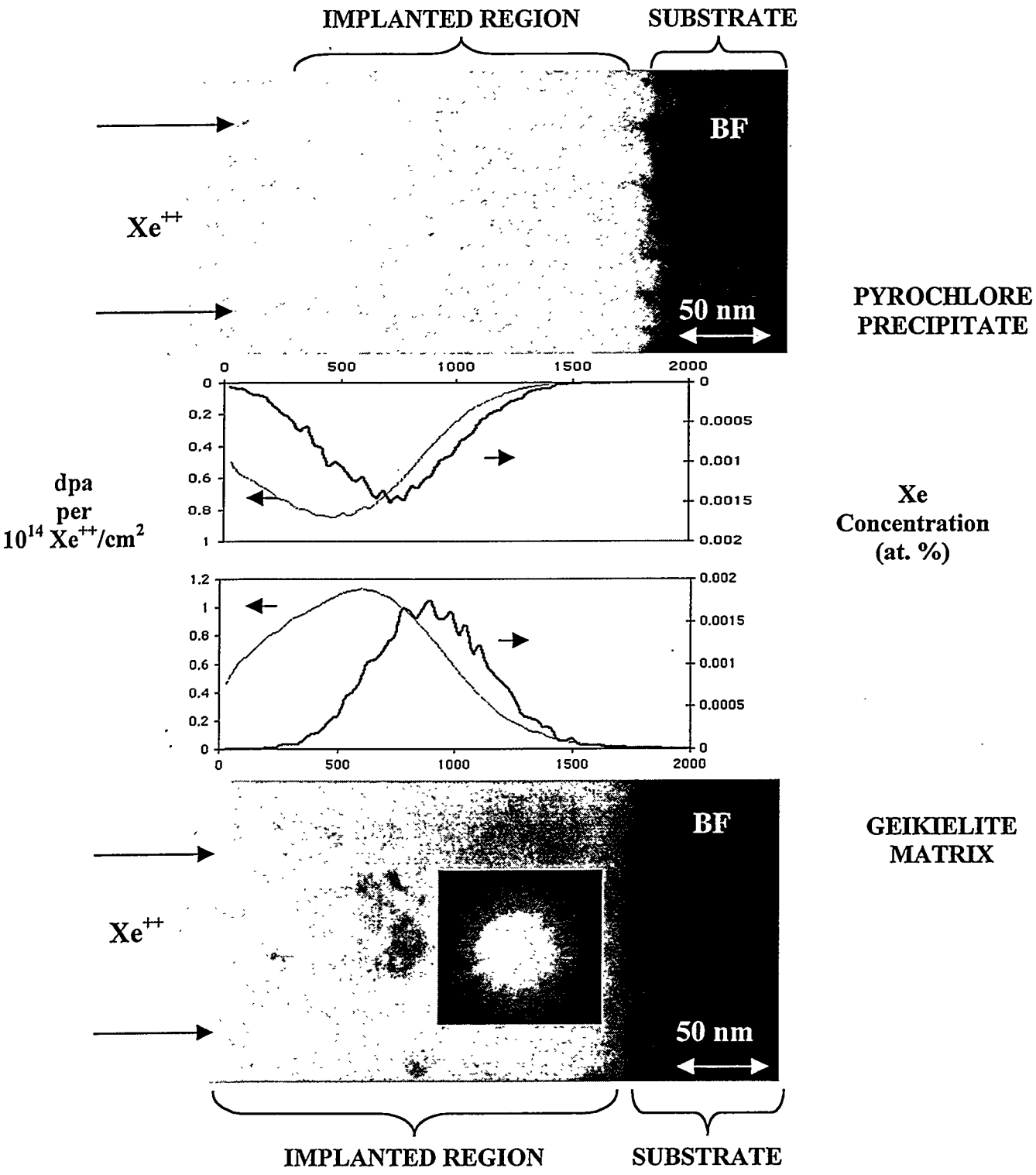

Figure 1: Transmission electron microscopy (TEM) bright-field (BF) images obtained from an $MgTiO_3 - Er_2Ti_2O_7$ composite sample irradiated with 350 keV Xe^{++} ions (top BF image from an $Er_2Ti_2O_7$ pyrochlore precipitate; bottom BF image from a region of

$MgTiO_3$ geikielite matrix; bottom inset microdiffraction pattern from a region of geikielite matrix) (ion fluence = 5×10^{14} Xe^{++}/cm^2; irradiation temperature = 100 K). Also shown are results of Monte Carlo simulations (based on the computer code TRIM) showing the range of 350 keV Xe^{++} ions in $MgTiO_3$ and $Er_2Ti_2O_7$, respectively, as well as displacement damage distributions for Xe ions in both oxide phases.

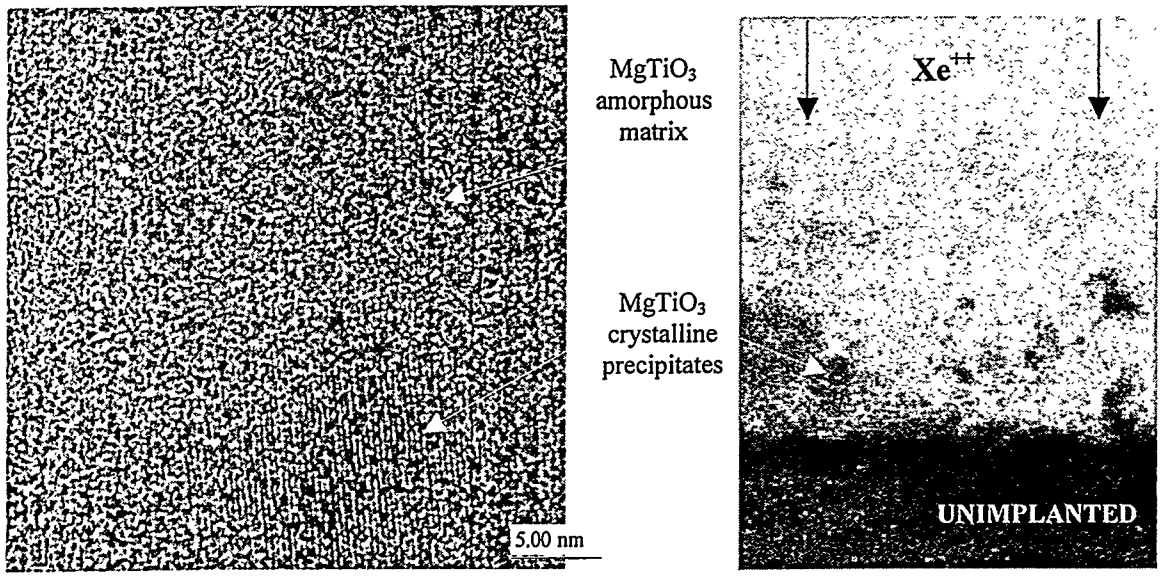

Figure 2: (a) High-resolution transmission electron microscopy (HRTEM) image and (b) cross-sectional TEM image obtained from a region of $MgTiO_3$ phase in an $MgTiO_3$ – $Er_2Ti_2O_7$ composite sample (same sample as in Fig. 1 irradiated with 350 keV Xe^{++} ions to. a fluence of 5×10^{14} Xe^{++}/cm^2 at 100 K. At this dose, the irradiated $MgTiO_3$ consists of isolated crystalline regions in an amorphous matrix.

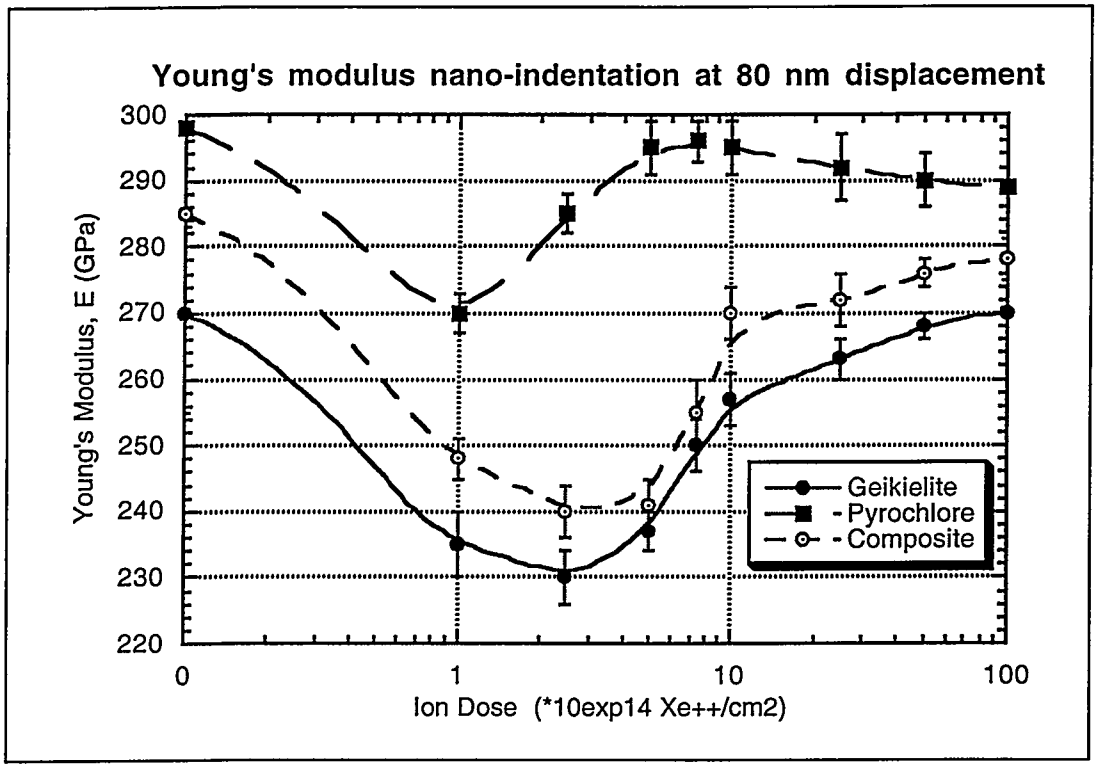
Young's modulus nano-indentation at 80 nm displacement
Young's Modulus, E (GPa)
300
290
280
270
260
250
240
230
220
0
1
10
100
Ion Dose (*10exp14 Xe++/cm2)
Geikielite
Pyrochlore
Composite

(a)

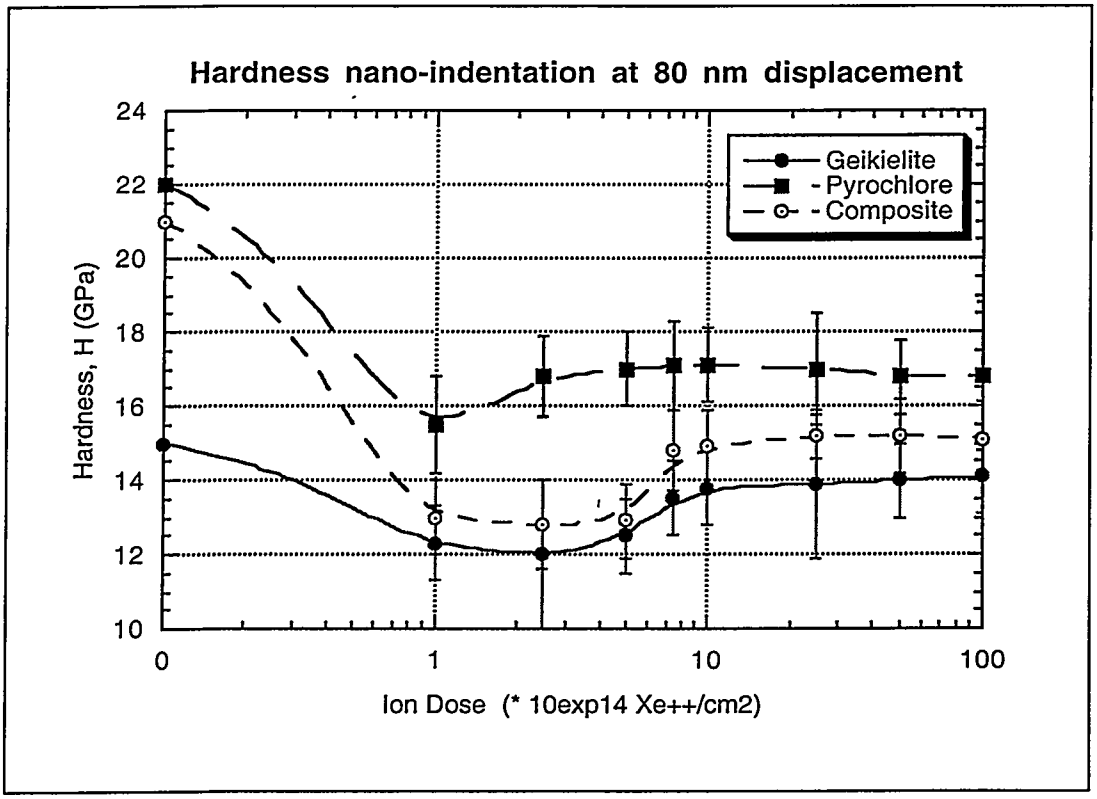
Hardness nano-indentation at 80 nm displacement
Hardness, H (GPa)
24
22
20
18
16
14
12
10
0
1
10
100
Ion Dose (* 10exp14 Xe++/cm2)
Geikielite
Pyrochlore
Composite

(b)

Figure 3: (a) Young's modulus (E) and (b) hardness (H) as a function of 350 keV Xe^{++} ion fluence for three different samples: (1) $MgTiO_3$ (Geikieliete); (2) $Er_2Ti_2O_7$ (Pyrochore) and (3) an $MgTiO_3$ - $Er_2Ti_2O_7$ composite sample. Measurements were made using the nanoindentation technique with an 80 nm indenter displacement.